Clinical and Experimental Medicine (2025) 25:147
https://doi.org/10.1007/s10238-025-01692-1

RESEARCH

Identification and construction of a novel NET-related gene signature for predicting prognosis in multiple myeloma

Haotian Yan[1,2] · Yangyang Ding[1,2] · Wenjie Dai[1,2] · Huiping Wang[1,2] · Hui Qin[1,2] · Zhimin Zhai[1,2] · Qianshan Tao[1,2]

Received: 14 January 2025 / Accepted: 14 April 2025

Abstract

Neutrophil extracellular traps are essential in the development and advancement of multiple myeloma (MM). However, research investigating the prognostic value with NET-related genes (NRGs) in MM has been limited. Patient transcriptomic and clinical information was sourced from the gene expression omnibus database. Cox regression analysis with a univariate approach was employed to explore the link between NRGs and overall survival (OS). Kaplan–Meier methods were applied to assess variations in survival rates. A nomogram integrating clinical data and predictive risk metrics was crafted using multivariate logistic and Cox proportional risk model regression analyses. Additionally, we investigated the disparities in biological pathways, drug sensitivity, and immune cell involvement, and validated differential levels of two key genes through qPCR. We identified 148 differentially expressed NRGs through published articles, of which 14 were associated with prognosis in MM. Least absolute shrinkage and selection operator Cox regression model established a nine-gene NRG signature—comprising ANXA1, ANXA2, ENO1, HIF1A, HSPE1, LYZ, MCOLN3, THBD, and FN1—that demonstrated strong predictive power for patient survival. The Cox regression model with multiple variables demonstrated that the risk score independently predicted OS, showing that those with a high score had worse survival rates. Furthermore, a nomogram incorporating patient age, LDH levels, the International Staging System, and NRGs was developed, demonstrating strong prognostic prediction capabilities. Drug sensitivity correlation analysis also offered valuable guidance for future immuno-oncological therapies and drug selection in MM patients. The NRGs signature was a reliable biomarker for MM, effectively identifying high-risk patients and forecasting clinical outcomes.

Keywords Multiple myeloma · Neutrophil extracellular traps · Prognostic signature · Tumor prognostic biomarkers

Abbreviations

R-ISS	Revised international staging system
OS	Overall survival
qPCR	Quantitative PCR
NLR	Neutrophil-to-lymphocyte ratio
NETs	Neutrophil extracellular traps
NRGs	NETs-related genes
GEO	Gene expression omnibus
LASSO	Least absolute shrinkage and selection operator
GSEA	Gene set enrichment analysis
MSigDB	Molecular signature database
ROCs	Receptor operating characteristic curves
ssGSEA	Single-sample genome set enrichment analysis
IC50	Inhibitory concentration in half
cDNA	Complementary DNA
t-SNE	T-distributed stochastic neighbor embedding
BMMCs	Bone marrow mononuclear cells

Haotian Yan and Yangyang Ding have equally contributed to this study.

✉ Zhimin Zhai
zzzzm889@163.com

✉ Qianshan Tao
ahmutqs@126.com

[1] Department of Hematology, The Second Affiliated Hospital of Anhui Medical University, Hefei 230601, Anhui, China

[2] Center of Hematology Research, Anhui Medical University, Hefei 230601, Anhui, China

Introduction

Plasma cell malignancy known as multiple myeloma (MM) is the second most prevalent type of hematological malignancy [1]. The traditional Durie–Salmon staging system (DS) and the revised international staging system (R-ISS) remain the most widely utilized prognostic classification

Published online: 09 May 2025

frameworks [2]. Currently, there is a lack of clear standards for the prognostic stratification system of R-ISS stage II multiple myeloma (MM) patients. Additionally, patients within the same stage may show varying clinical outcomes due to pronounced tumor heterogeneity and the presence of subclones, both interpatient and intrapatient [3, 4]. Despite some advances in treatment, the majority of patients with MM remain largely incurable, but overall survival (OS) has improved significantly over the last decade, even though the disease remains incurable [5]. Most patients continue to face drug-resistant relapses posttreatment. Therefore, the development of novel prognostic markers is crucial.

The human immune system primarily relies on neutrophils as the dominant effector cells of innate immunity. Increasing evidence suggests that circulating and infiltrating neutrophils are implicated in various aspects of tumorigenesis and progression [6]. Cancer patients' prognosis is independently predicted by the neutrophil-to-lymphocyte ratio (NLR) [7]. In hematological malignancies, elevated levels of neutrophil extracellular traps (NETs) correlate with lymphoma advancement and the development of pediatric acute leukemia [7]. In the tumor microenvironment, neutrophils demonstrate significant plasticity in response to polarization and activation signals, leading to both direct and indirect cancer-promoting mechanisms [8]. In MM, tumor-related neutrophils facilitate myeloma cell survival, proliferation, and resistance to therapy [9]. Neutrophil defense mechanisms include not only the engulfment of pathogens, the release of granules, and the secretion of cytokines but also the creation of NETs, which subsequently eliminate pathogens [10]. Recent research indicates that MM patients displaying elevated NETs in plasma or tumor tissue exhibit worse prognosis [11, 12]. However, studies exploring the association between NET-related genes (NRGs) and MM prognosis remain scarce.

This research focused on identifying NRGs and analyzed their association with MM prognosis. Univariate Cox and LASSO regressions were applied to the training cohort to develop NRG-based prognostic signature, which were subsequently validated in an external cohort. Calibration curves were employed for assessing the precision associated with the nomogram. Furthermore, we compared drug sensitivity, immune infiltration, and pathway differences between the two groups. Our objective was to highlight the pivotal role played by NRGs in assessing the prognosis of MM patients through comprehensive genomic analysis and to provide guidance to clinical decision makers.

Materials and methods

Data acquisition and analysis

Clinical records and NRG-related information from MM patients were sourced from the gene expression omnibus (GEO) database. The GSE2658 dataset, encompassing 559 MM patients, served as the training dataset. GSE136337 containing 426 MM patients was used as an independent validation dataset. Table 1 summarizes clinical profiles of MM patients across the different datasets.

Obtaining a list of NRGs

NRGs are mainly cited from relevant research advances and articles. Previously published NRGs were manually curated from the literature, resulting in the inclusion of 148 identified NRGs for further analysis, as detailed in Supplementary Table S1 [13].

Table 1 Clinical parameter characteristics of the MM patients retrieved from the GEO databases

Characteristics		GSE2658	GSE136337	GSE9782
Category		Training cohort	Validation cohort	Validation cohort
Platform		GPL570	GPL27143	GPL96
Total number		559	426	264
Survival status	Survival	459(82.1%)	243(57.0%)	109(41.3%)
	Death	100(17.9%)	183(43.0%)	155(58.7%)
Age	> 65	126(22.5%)	119(27.9%)	80(30.3%)
	≤ 65	433(77.5%)	307(72.1%)	184(69.7%)
Sex	Male	336(60.1%)	261(61.3%)	159(60.2%)
	Female	223(39.9%)	165(38.7%)	105(39.8%)
ISS	I	318(56.9%)	170(39.9%)	69(26.1%)
	II	121(21.6%)	135(31.7%)	64(24.2%)
	III	120(21.5%)	121(28.4%)	61(23.1%)
	Unknown	–	–	70(26.5%)

Analysis of annotation functions

Gene set enrichment analysis (GSEA) was conducted with the "clusterProfiler" tool. The GSEA employed gene sets from the molecular signature database (MSigDB), including the c2.cp.kegg.v2023.1.Hs.entrez and c5.go.bp.v2023.1.Hs.entrez compilations, accessible at https://www.gseamsigdb.org/gsea/msigdb/index.jsp. Permutations were determined at 1,000; the p value criterion for pinpointing statistically meaningful connections was set at less than 0.05.

Identification of NRGs linked to overall survival (OS)

GSE2658 and GSE136337 datasets were categorized into training and validation subsets. To identify NRGs linked to OS in the training set ($p < 0.05$), univariate Cox regression analysis was employed.

Development and validation of an NRG-based predictive signature for MM patients

LASSO regression was utilized to filter the training dataset for identifying NRGs that forecast MM prognostic indicators. The LASSO technique was applied to create the NRGs signature from the GEO data, defining the risk score signature accordingly:

$$\text{Riskscore} = \sum_{i=1}^{N} (\exp \times \text{coef})$$

where N denotes the count of signature genes; exp denotes the level of gene expression; and coef refers to the index of coefficient. The predictive power of the prognostic signature was assessed through Kaplan–Meier survival curves and receiver operating characteristic curves (ROC) curves, tracked over time. NRGs' column plots were generated with "rms" software and their efficacy was evaluated through curve calibration.

Immune infiltration assessment

The single-sample genome set enrichment analysis (ssGSEA) algorithm was run using the "GSVA" software to determine the levels and functions of immune cells infiltrating tumors in patients who were classified as either high or low risk. The results were subsequently illustrated using the "vioplot" software package.

Assessment of treatment reactivity

Assessment of chemotherapy responsiveness between high- and low-risk categories involved the "pRRophetic" software package, specifically version 0.5. This software tool models ridge regression derived from gene expression data and applied tenfold cross-validation to predict half-maximal inhibitory concentration (IC50) values. The "pRRophetic" package's dataset, sourced from the "cgp2016" study, contains gene expression and drug treatment records for 251 medications and 13 myeloma cell types. Standard anticancer agents like bortezomib, bleomycin, and etoposide, along with other medications, were evaluated using their clinical track records. Box plots were used to depict the varying degrees of drug responsiveness among high-risk and low-risk patient groups.

Patient samples

A total of 13 newly diagnosed MM patients, 7 in complete remission, 7 with relapsed/refractory MM, and six healthy controls were included, from whom bone marrow samples were obtained at the Second Affiliated Hospital of Anhui Medical University. Institutional approval was obtained from Anhui Medical University's Second Affiliated Hospital Ethics Committee, with consent provided by all participants after adequate information was imparted. All procedures were performed following the appropriate protocols and ethical standards. A density gradient centrifugation method was used to isolate the fraction containing lymphocytes and monocytes from bone marrow samples for subsequent experiments.

Quantitative PCR (qPCR)

RNA extraction from the cells was conducted with the SteadyPure Rapid RNA Extraction Kit (Genuine, China), adhering to the manufacturer's guidelines. Following this, complementary DNA (cDNA) synthesis was achieved using the Thermo Scientific Specific Reverse Transcription Kit (Catalog No. K1691). Quantitative analysis of gene activity involved the SYBR Premix Ex Taq (Takara) kit, with GAPDH serving as a reference. After an initial denaturation at 95 °C for 30 s, the amplification proceeded with 40 cycles of 95 °C for 5 s and 60 °C for 30 s. Melt curve analysis comprised a denaturation phase at 95 °C for 15 s, an annealing phase at 60 °C for 60 s, and a cooling phase at 50 °C for 30 s. The primers for HSPE1, MCOLN3, and GAPDH are specified below: HSPE1 has a forward primer of 5'-ATGGCA GGACAAGCGTTTAGA and a reverse primer of 5'-TGG AAGCATAATGCCTCCTTTG. For MCOLN3, the forward primer reads *5'-CTCCGTTGGGAATCATGCTTAT*, with the reverse being *5'-GATGTTTCCTCGCTTGTAGAAGT*. Lastly, the GAPDH primers consist of a forward sequence of *5'-AGCAAGAGCACAAGAGGAAG* and a reverse sequence of *5'-GGTTGAGCACAGGGTACTTT*.

Statistical analysis

All statistical analyses utilized R software (version 4.2.1). The t test was utilized to evaluate the differences in continuous variables with a normal distribution between the two groups. The log-rank test was used to compare survival curves generated by the Kaplan–Meier method. Genes associated with MM prognosis were identified using univariate Cox regression. A predictive signature was then developed utilizing LASSO regression analysis. This research employed two-tailed p values, with a threshold of $p < 0.05$ marking statistical significance.

Results

Modeling NRGs prognostic signature

Through a comprehensive literature review, we identified a total of 148 genes associated with neutrophil extracellular traps (NETs). To further investigate their prognostic relevance in multiple myeloma (MM), we conducted a univariate Cox regression analysis using the training dataset GSE2658. Applying a significance threshold of $p < 0.05$, we identified 14 candidate genes that exhibited a statistically significant association with MM prognosis. These genes include ANXA1, ANXA2, CLEC7A, ENO1, ENTPD4, HIF1A, HSPE1, IL17A, LYZ, MCOLN3, PKM, THBD, VIM, and FN1 (Fig. 1A). Prognostic features were constructed using a tenfold cross-validated LASSO Cox regression, which identified an optimal prognostic feature comprising nine genes with nonzero coefficients: ANXA1, ANXA2, ENO1, HIF1A, HSPE1, LYZ, MCOLN3, THBD, and FN1. This characteristic was identified when the model attained the lowest λ (lambda) value (Fig. 1B–C). The risk score is calculated by multiplying ANXA1 expression by 0.00046, ANXA2, and ENO1 by 0.38816, HIF1A by 0.02071, HSPE1 by 0.15562, LYZ by -0.00855, MCOLN3 by 0.07044, THBD by -0.09367, and FN1 by 0.03190, then adding them all together.

Participants in the training group were grouped according to risk scores (Fig. 2A). With the median risk assessment, individuals were categorized into a high-risk category (comprising 279) and a low-risk category (comprising 280). A clear pattern indicated that elevated risk scores correlated with higher mortality, as high-risk individuals demonstrated a substantially worse prognosis compared to low-risk individuals (Fig. 2A–B). Kaplan–Meier survival curves also confirmed this difference (Fig. 2E). Downscaled PCA, along with t-distributed stochastic neighbor embedding (t-SNE), revealed distinct patient profiles across different risk categories (Fig. 2C–D). We also examined the ability to predict survival rates over 3 and 5 years through the use of risk scores. Figure 2F illustrates ROC curves with area under curve (AUC) of 0.601 and 0.615 for the training set ($p < 0.05$, DeLong's test). These findings indicate that risk scores serve as dependable indicators of long-term survival for patients with MM.

Verification of predictive signature in validation cohort

We employed the GSE136337 dataset as our validation group and consistently observed that patients identified as high-risk—using the same calculation method applied in the training cohort—demonstrated markedly poorer outcomes within the GSE136337 validation cohort (Fig. 3A, E). The patterns of elevated risk and mortality aligned with those seen in the training cohort (Fig. 3B). PCA and t-SNE methodologies demonstrated a clear two-way distinction among patients within

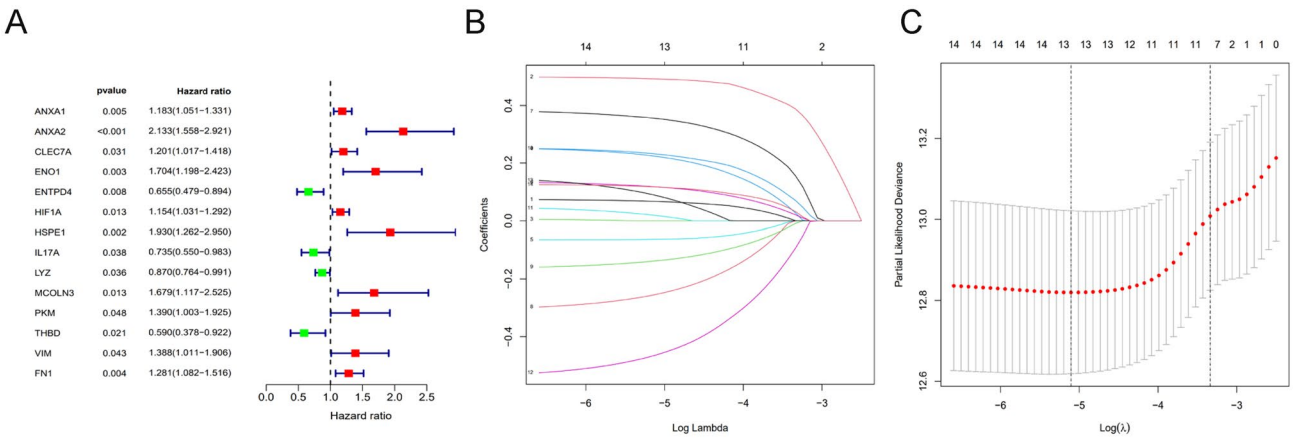

Fig. 1 Determination of prognostic NRGs and construction of prognostic models. **A** Forest plots of univariable Cox model. **B** LASSO coefficient profiles of the expression of ten candidate genes. **C** Selection of the optimal gene in the Lasso model (λ)

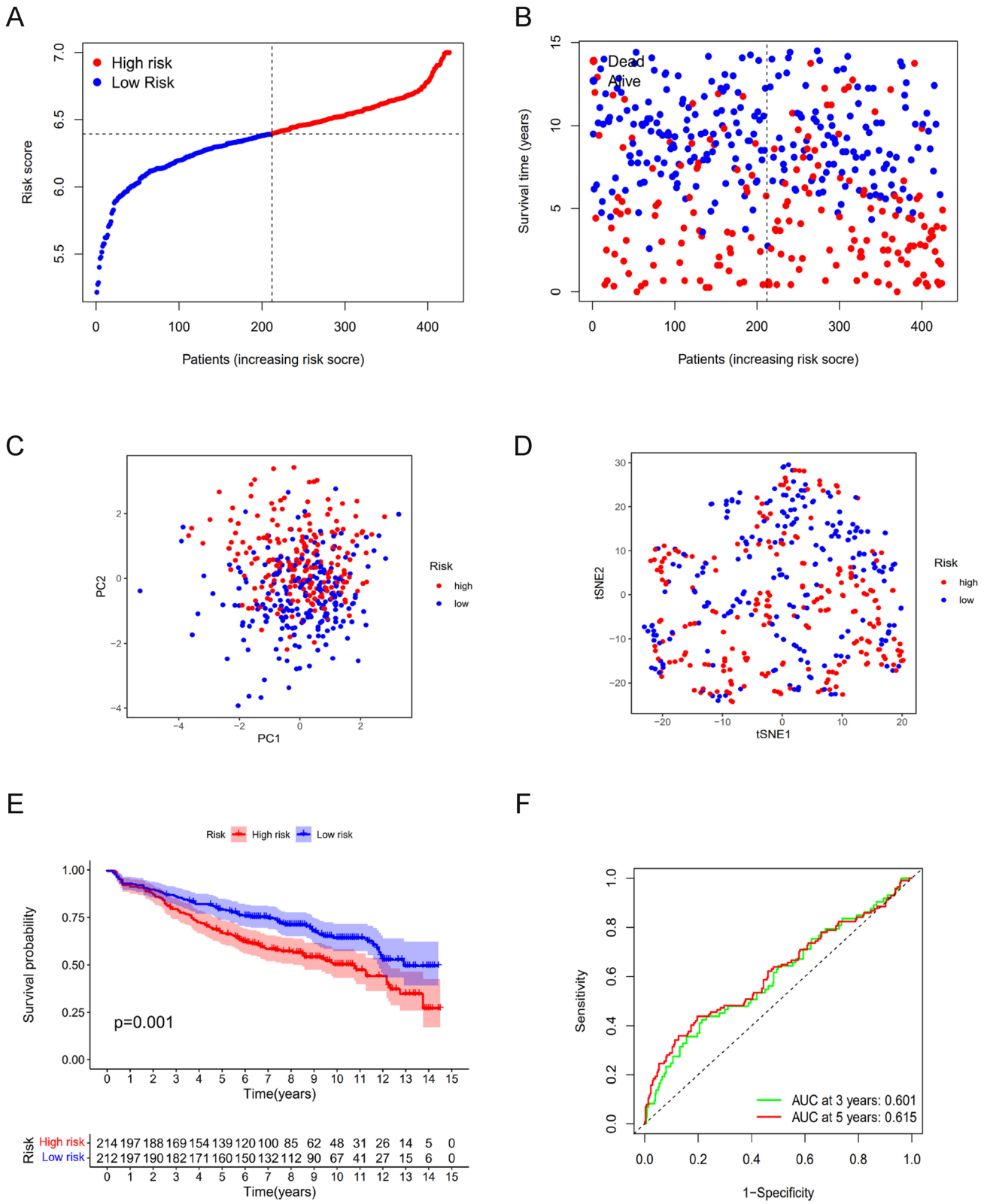

Fig. 2 Prognostic analysis of the eight-gene signature in the training cohort. **A** The distribution and median value of the risk scores in the training cohort. **B** The distributions of OS status, OS time, and risk score in the training cohort. **C** PCA plots of the GEO database training cohort population. **D** t-SNE analysis of the training cohort population. **E** Kaplan–Meier curves of OS for patients in the high-risk and low-risk groups of the training cohort. **F** UC of time-dependent ROC curves verified the prognostic performance of the risk score in the training cohort

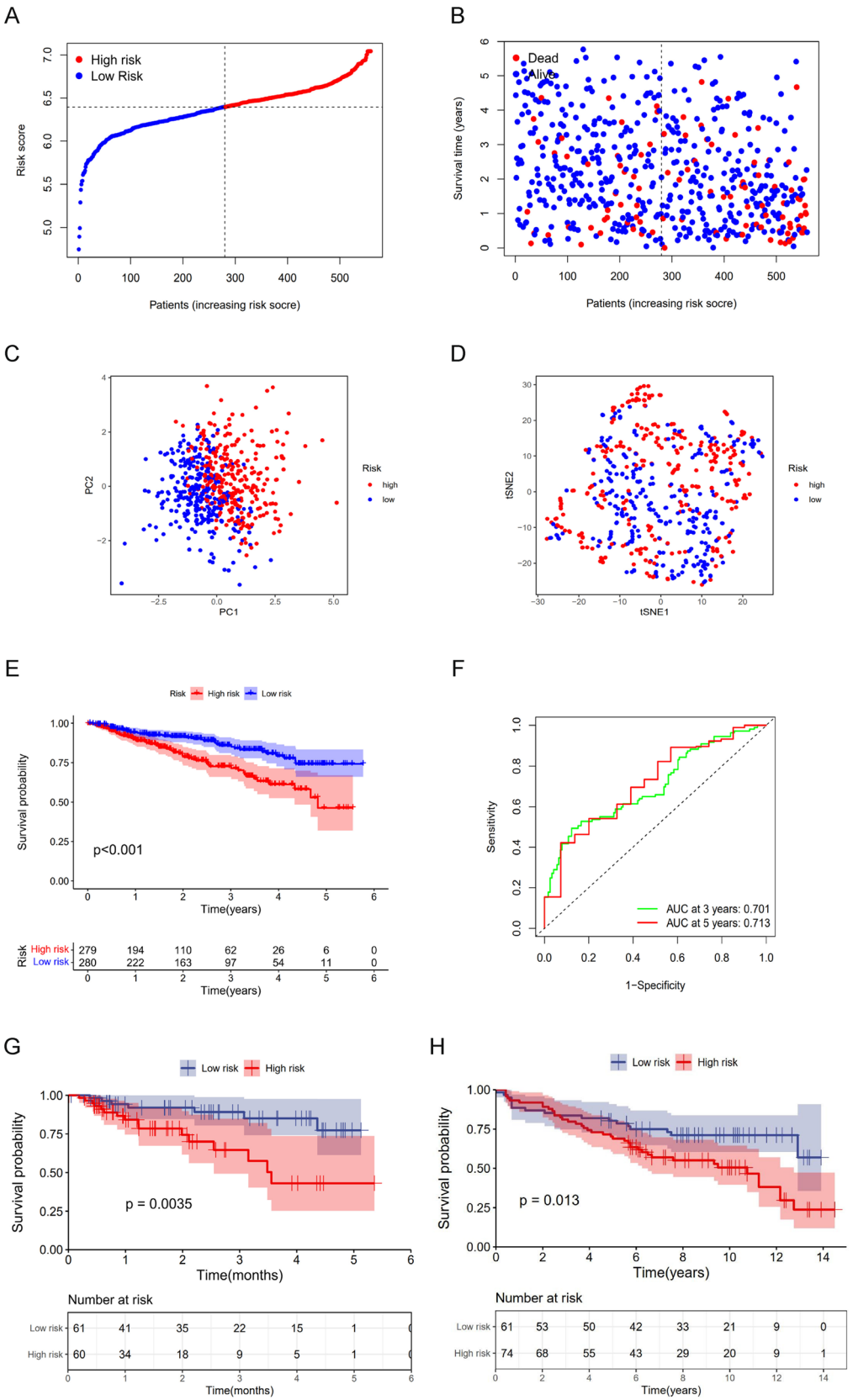
A
High risk
Low Risk
Risk score
Patients (increasing risk socre)
B
Dead
Alive
Survival time (years)
Patients (increasing risk socre)
C
PC2
PC1
Risk
high
low
D
tSNE2
tSNE1
Risk
high
low
E
Risk High risk Low risk
Survival probability
p<0.001
Time(years)
Risk High risk 279 194 110 62 26 6 0
Low risk 280 222 163 97 54 11 0
Time(years)
F
Sensitivity
1−Specificity
AUC at 3 years: 0.701
AUC at 5 years: 0.713
G
Low risk High risk
Survival probability
p = 0.0035
Time(months)
Number at risk
Low risk 61 41 35 22 15 1
High risk 60 34 18 9 5 1
Time(months)
H
Low risk High risk
Survival probability
p = 0.013
Time(years)
Number at risk
Low risk 61 53 50 42 33 21 9 0
High risk 74 68 55 43 29 20 9 1
Time(years)

◂**Fig. 3** Validation of the eight-gene signature in the validation cohort. **A** Distribution and median values of risk scores in the validation cohort. **B** Validate the distribution of OS status, OS time, and risk score in the queue. **C** PCA plots of the validation cohort population. **D** t-SNE analysis of the validation cohort population. **E** Kaplan–Meier curves of OS for patients in the high-risk and low-risk groups of the validation cohort. **F** AUC of time-dependent ROC curves in the validation cohort. **G** Kaplan–Meier curves of OS for stage II MM patients in the training cohort. **H** Kaplan–Meier curves of OS for stage II MM patients in the validation cohort

different risk groupings (Fig. 3C–D). Within the validation cohort, the AUC for risk assessments in forecasting 3-year and 5-year mortality rates stood at 0.701 and 0.713, respectively ($p < 0.05$, DeLong's test) (Fig. 3F). The current R-ISS staging system enhances the ISS staging, offering better differentiation of outcomes in MM patients. Given the challenges in distinguishing stage II MM patients, we investigated the prognostic significance of the NRGs signature in this stage [14, 15]. Kaplan–Meier curves revealed that high-risk patients had notably poorer OS than low-risk patients in both the training and validation groups (Fig. 3G–H). This implies that the signature could be a valuable addition to the current staging system, facilitating more accurate stratification of MM patients.

Construction of prognostic prediction nomograms

In the univariate and multivariate Cox regression analyses conducted on the training and validation datasets depicted in Figs. 4A–D, it was determined that age, ISS, and the risk score emerged as robust, standalone indicators of the prognosis for MM. Based on these results, we created a nomogram that incorporates patient age, ISS, and the combined risk score (Fig. 4E). The nomogram was utilized to calculate the OS rates for MM patients at 1 year, 3 years, and 5 years. Calibration curves showed that signature accurately predicted disease progression and enabled personalized prognostic evaluations for MM patients (Fig. 4F). On the training dataset, the ROC values of the nomogram for the prediction of 1-year, 3-year, and 5-year overall survival were 0.690, 0.714, and 0.757, respectively, which outperformed the ROC values of the other individual metrics for each year (Figs. 4G–I), and the validation dataset showed the same trend, with the ROC values of the prediction of 1-year, 3-year, and 5-year overall survival of 0.742, 0.678, and 0.692, respectively (Figs. 4J–L), suggesting the advantage of our nomogram over other factors. The nomogram emerges as a reliable indicator for predicting the prognosis of MM.

Immune infiltration status within the training cohort

To determine the variance in immune cell infiltration across the two risk categories, the ssGSEA method was utilized to assess the abundance of diverse immune cell subsets and associated pathways. In the training cohort, immune cells such as Th1 and Treg had lower performance scores in the high-risk group than in the low-risk group (Fig. 5A). Significantly, the largest discrepancy in scores was observed among Treg cells across the two risk groups. Compared to the low-risk group, the high-risk group had significantly lower scores in the domains of CCR metrics, checkpoint molecules, T cell synergistic inhibition, T cell synergistic stimulation, and type I interferon response (Fig. 5B).

Genome enrichment analysis

To explore the impact of these 9 NRGs in MM disease progression, we performed GSEA with the aim of revealing commonalities and differences in tumor-related signaling pathways between high- and low-risk patients. The GO analysis highlighted significant enhancement in pathways pertinent to AMP biosynthesis, DNA strand separation during replication, kinetochore organization, and the elongation of the mitotic spindle among those with high NRG expression. Conversely, the group with minimal exhibited an enhancement in pathways such as the mucosal innate immune response, organization of lysosomal membranes, positive modulation of neuroinflammatory responses, the noncanonical Wnt signaling pathway, and the oversight of microglial cell activation (Fig. 6A–B). The KEGG analysis demonstrated that the group with high expression levels exhibited a notable abundance across multiple pathways, such as aminoacyl tRNA biosynthesis, base excision repair, DNA replication, mismatch repair, and the one-carbon metabolism involving folate. Additionally, several immune-related pathways, such as B-cell receptor signaling, interactions between cytokine receptors, and neuroactive ligand–receptor interactions, showed varying levels of enrichment in the group with low NRG expression (Fig. 6C–D).

Role of risk scores in drug susceptibility correlation analysis and immunotherapy

Chemotherapy is the traditional regimen for MM treatment, but clinical resistance remains inevitable. To identify potential therapeutic agents, we conducted a drug sensitivity correlation analysis using a training set of MM patients, stratified by high-risk and low-risk subgroups. The study included eight conventional chemotherapeutic agents: bortezomib, bleomycin, etoposide, vincristine, dasatinib, doxorubicin, imatinib, and lukotinib. The findings revealed that patients with higher scores appeared to be more responsive to bortezomib, bleomycin, and dasatinib, whereas low-score patients exhibited sensitivity to etoposide, vincristine, imatinib, and ruxolitinib.

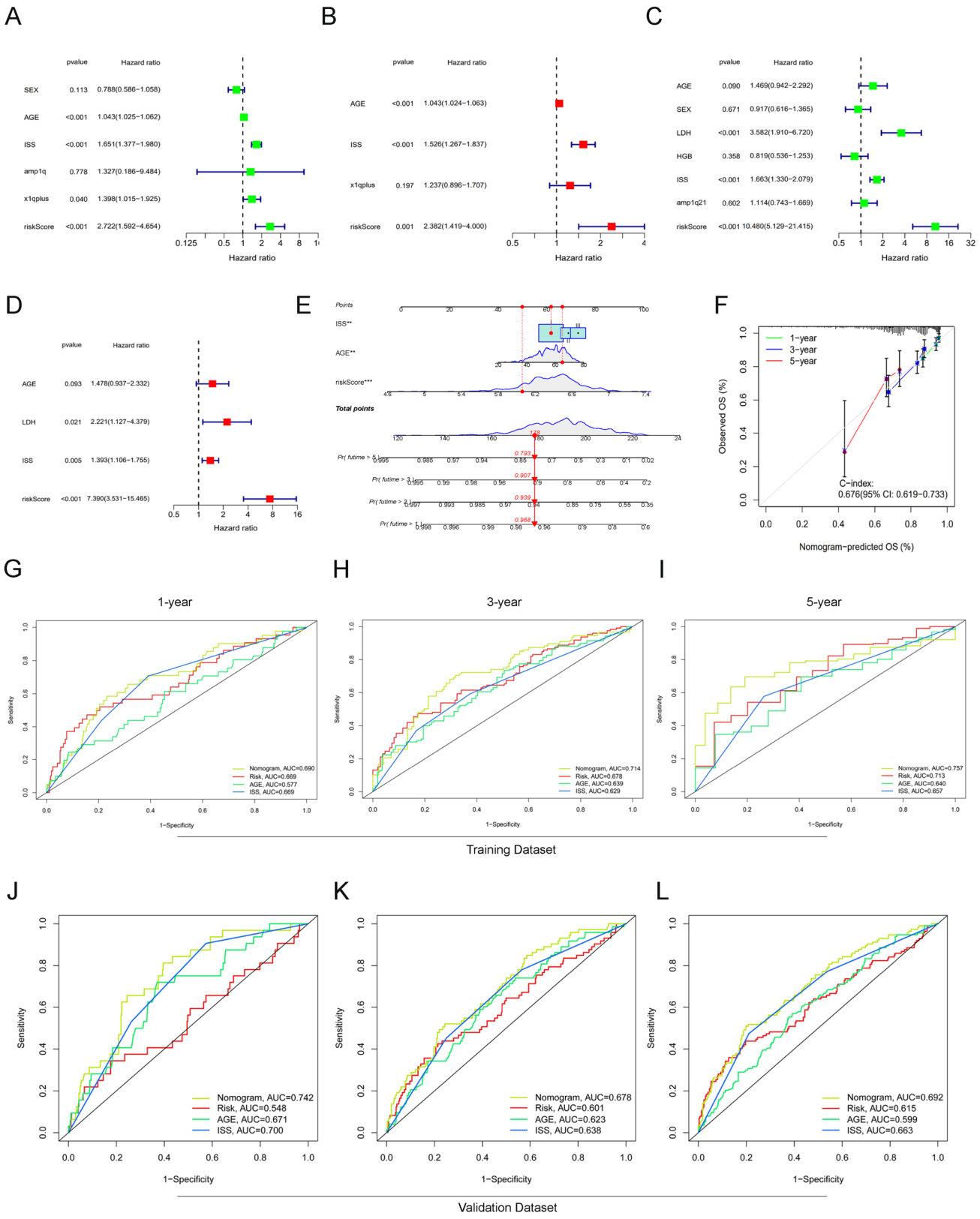
A
pvalue Hazard ratio
SEX 0.113 0.788(0.586−1.058)
AGE <0.001 1.043(1.025−1.062)
ISS <0.001 1.651(1.377−1.980)
amp1q 0.778 1.327(0.186−9.484)
x1qplus 0.040 1.398(1.015−1.925)
riskScore <0.001 2.722(1.592−4.654)
Hazard ratio
B
pvalue Hazard ratio
AGE <0.001 1.043(1.024−1.063)
ISS <0.001 1.526(1.267−1.837)
x1qplus 0.197 1.237(0.896−1.707)
riskScore 0.001 2.382(1.419−4.000)
Hazard ratio
C
pvalue Hazard ratio
AGE 0.090 1.469(0.942−2.292)
SEX 0.671 0.917(0.616−1.365)
LDH <0.001 3.582(1.910−6.720)
HGB 0.358 0.819(0.536−1.253)
ISS <0.001 1.663(1.330−2.079)
amp1q21 0.602 1.114(0.743−1.669)
riskScore <0.001 10.480(5.129−21.415)
Hazard ratio
D
pvalue Hazard ratio
AGE 0.093 1.478(0.937−2.332)
LDH 0.021 2.221(1.127−4.379)
ISS 0.005 1.393(1.106−1.755)
riskScore <0.001 7.390(3.531−15.465)
Hazard ratio
E
Points
ISS**
AGE**
riskScore***
Total points
F
1−year
3−year
5−year
C−index:
0.676(95% CI: 0.619−0.733)
Observed OS (%)
Nomogram−predicted OS (%)
G
1-year
Nomogram, AUC=0.690
Risk, AUC=0.669
AGE, AUC=0.577
ISS, AUC=0.669
H
3-year
Nomogram, AUC=0.714
Risk, AUC=0.678
AGE, AUC=0.639
ISS, AUC=0.629
I
5-year
Nomogram, AUC=0.757
Risk, AUC=0.713
AGE, AUC=0.640
ISS, AUC=0.657
Sensitivity
1−Specificity
Training Dataset
J
Nomogram, AUC=0.742
Risk, AUC=0.548
AGE, AUC=0.671
ISS, AUC=0.700
K
Nomogram, AUC=0.678
Risk, AUC=0.601
AGE, AUC=0.623
ISS, AUC=0.638
L
Nomogram, AUC=0.692
Risk, AUC=0.615
AGE, AUC=0.599
ISS, AUC=0.663
Validation Dataset

◂**Fig. 4** Results of the univariate and multivariate Cox regression analyses regarding OS and construction of a nomogram. **A** Results of univariate Cox regression analysis of the GSE2658 training cohort. **B** Results of multivariate Cox regression analysis of the GSE2658 training cohort. **C** Univariate Cox regression analysis of the GSE136337 validation cohort. **D** Multivariate Cox regression analysis of the GSE136337 validation cohort. **E** Construction of the nomogram. **F** Calibration plot used to predict the 1-, 3-, and 5-year survival. **G–I** ROCs for 1-, 3-, and 5-year eigenfactors in the training cohort. **J–L** ROC for 1-, 3-, and 5-year eigenfactors in the validation cohort

No significant variation in doxorubicin sensitivity was observed between the groups. The results suggest that the risk score could act as a measure of how sensitive individuals are to drugs, reinforcing the idea that those in the high-risk category typically exhibit lower sensitivity to chemotherapy than their low-risk counterparts (Fig. 7, 8A–H).

HSPE1 and MCOLN3 are highly expressed in newly diagnosed and relapsed/refractory MM patients

To enhance the confirmation of two particular NRGs, we conducted qPCR on human bone marrow mononuclear cells (BMMCs). In contrast to healthy controls (IDA), individuals with newly diagnosed MM (ND) and those experiencing relapsed or refractory MM (R/R) exhibited significantly increased expression levels of HSPE1 and MCOLN3. However, there was no significant variation found in the remission group (CR). Additionally, HSPE1 and MCOLN3 expression levels were markedly elevated in the ND and R/R groups relative to the CR group (Fig. 9A–B).

Discussion

Multiple myeloma (MM) is a plasma cell malignancy, accounting for approximately 10% of hematologic cancers. It usually advances from the premalignant phase of asymptomatic clonal plasma cell hyperplasia and remains untreatable, mainly because of drug resistance and disease relapse [16, 17]. This highlights the critical necessity to establish dependable biomarkers for improved prognostic evaluation. In this study, we analyzed the prognostic relevance of NRGs in MM patients. We created a prognostic signature for risk using nine OS-related NRGs, which demonstrated effective prognostic capability. The current R-ISS staging system has refined the ISS system to better distinguish the prognosis of MM patients. However, there remains a significant survival disparity among patients classified as stage II, which warrants clinical attention. Numerous researchers have been striving to enhance the R-ISS staging system. Our prognostic model has notably improved the identification of MM patients, particularly those in stage II. Furthermore, we confirmed the expression of two of these genes through qPCR, producing results of possible research significance. These findings suggest that our data are reliable and hold significant research promise. In summary, our research has uncovered a new and dependable NRGs prognostic signature for MM patients.

The nine-gene framework we developed enables a more accurate classification of individuals into high-risk and low-risk groups, demonstrating exceptional consistency and dependability across both our training and validation datasets. Specifically: (1) patients across various risk categories can be distinctly identified; (2) individuals in the high-risk subgroup display a poorer prognosis; (3) stage II MM is more clearly differentiated between high-risk and low-risk subgroups; and (4) the signature has strong diagnostic value for predicting long-term survival. These findings support our hypothesis that NRGs may serve as novel prognostic markers for MM patients. Notably, compared to many existing MM studies that rely solely on gene-based models, our approach incorporates additional factors such as age and staging, representing a significant enhancement to the ISS scoring system. The validity of our proposed prognostic traits in predicting outcomes was further validated by the analysis of Kaplan-Meyer curves and the application of univariate and multivariate regression methods, especially in their predictive ability for patients with stage II multiple myeloma. This may provide a new avenue for improving the diagnostic approach to MM staging in the future.

In the training cohort, we used univariate regression and LASSO regression analyses to construct risk profiles for nine genes, aiming to evaluate the predictive capability of NRGs. This risk score serves as an independent predictive marker. In order to enhance the value of the features in clinical applications, we designed a nomogram that integrates patient clinical data alongside prognostic scores. Calibration curve analysis demonstrated the strong predictive capacity of this signature. This research is the inaugural evaluation of NRGs in multiple myeloma (MM). Notably, the NET-based risk signature is also applicable to other solid tumors. A prognostic model for hepatocellular carcinoma was developed using m6A and NET-related lncRNAs. In the training dataset, the AUC values for one, three, and five years were recorded at 0.740, 0.755, and 0.749, respectively. In a similar vein, the risk signature for pancreatic cancer NRGs demonstrated robust predictive capability, achieving AUCs values hitting 0.742, 0.748, and 0.809 for 2-year, 3-year, and 5-year outcomes, respectively [18]. Additionally, we compared our model with other prognostic models related to NETs. The study by Mo et al. established a prognostic model for NET-related lung adenocarcinoma, with AUC values of 0.685, 0.687, and 0.683 at 1, 3, and 5 years, respectively, demonstrating certain prognostic value. However, our model achieved AUC values of 0.601 and 0.615 at 3 and 5 years, respectively, showing a superior improvement over the

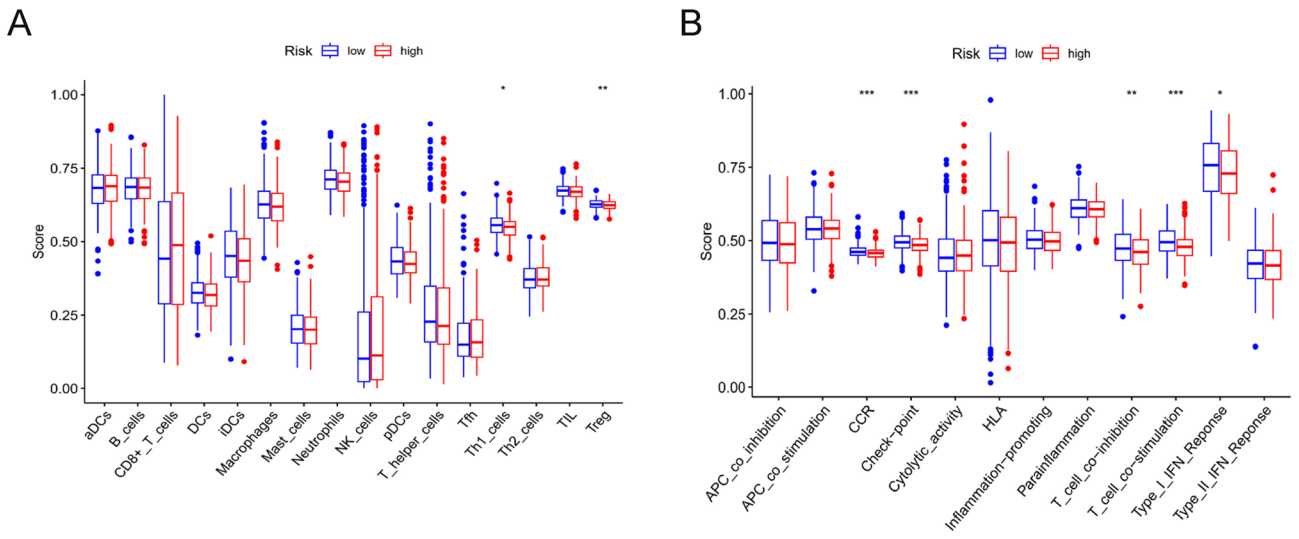

Fig. 5 Comparison of the ssGSEA scores between different risk groups. **A** Scoring of sixteen immune cell types in the training cohort. **B** Twelve immune-related functions of the GEO cohort. (aDC, Activated dendritic cell; iDC, Immature dendritic cell; pDC, Plasmacytoid dendritic cell; Tfh, T follicular helper cell; Th2, T helper 2; TIL, Tumor infiltrating lymphocyte; Treg, Regulatory T Cell; HLA, Human leukocyte antigen; APC, Antigen presenting cell; CCR, Cytokine–cytokine receptor; Adjusted p values were showed as: *, $p<0.05$, **, $p<0.01$, ***, $p<0.001$.)

aforementioned model [19]. Research indicates that NET-based prognostic signatures may offer valuable prognostic insights in the context of solid tumors.

Genes within the NRG risk signature play various roles across multiple diseases. Annexin A1 (ANXA1), the first identified protein in the annexin family, known for binding calcium ions and phospholipids, functions as a suppressor of both inflammation and immune responses. When its regulation is disrupted, it can drive the progression and spread of cancer [20]. For example, in a previous study, overexpression of ANXA1 resulted in tumors generating more blood vessels, which accelerated growth [21]. In addition, ANXA1 expression is closely associated with the differentiation status of epithelial cells, with downregulation of ANXA1 leading to incomplete differentiation of epithelial cells, and poorly differentiated tumors being more aggressive, with higher growth and recurrence rates [22]. ANXA2, commonly referred to as Annexin A2, is a protein that is ubiquitously expressed across various eukaryotic cell types. It has been implicated in driving the progression of multiple cancers, such as those affecting the esophagus [23], pancreatic [24], and gastric cancers [25]. Hypoxia-inducible factor HIF1A acts as a transcription factor, aiding tumor cells in adapting to low-oxygen conditions. Hypoxia is a prevalent characteristic of the tumor microenvironment across different cancer types [26], and the activation of relevant downstream signaling pathways during hypoxia can regulate tumor-specific immune responses, enabling immune escape and promoting tumor progression [27]. In addition, HIF1A can be a candidate target for recognizing MM miRNA regulation [28]. HSPE1, a heat shock protein family member, encodes the minor subunit of the mitochondrial HSP60/HSP10 chaperone complex [29]. Mucolipin 3 (MCOLN3) is part of the MCOLN/TRPML non-cationic channel, which functions as a calcium-permeable transporter [30]. Mucolipin 3 is expressed across various cellular compartments, including lysosomes, plasma membranes, autophagosomes, and early endosomes [31, 32]. Fibronectin 1 (FN1) is a large adhesion glycoprotein that constitutes a major component of the extracellular matrix. It can be secreted by various cells, including fibroblasts, chondrocytes, myoblasts, synoviocytes, and tumor cells [33]. Elevated FN1 expression impacts the outcomes of various cancers, including gastric [34] and breast cancer [35], and can be associated with immune infiltration as a prognostic marker. The last two genes are protective genes for MM. Lysozyme (LYZ) is a secreted protein with antimicrobial properties that is normally expressed in monocytes/macrophages [36]. Under specific conditions, increased activation of LYZ + myeloid cells may be a biomarker of intestinal inflammation [37]. Thrombomodulin (THBD) is part of the protein C anticoagulant system, influencing vascular endothelium and contributing to anti-inflammatory actions and barrier integrity [38]. Previous data from animal signatures have shown that THBD mutations have prothrombotic effects [39]. Many studies have shown that low expression of THBD during tumourigenesis enhances tumor cell invasion and proliferation in vitro, as shown in various examples: intrahepatic metastases and portal vein tumor thrombosis are more frequent in hepatocellular carcinoma with low THBD expression [40, 41].

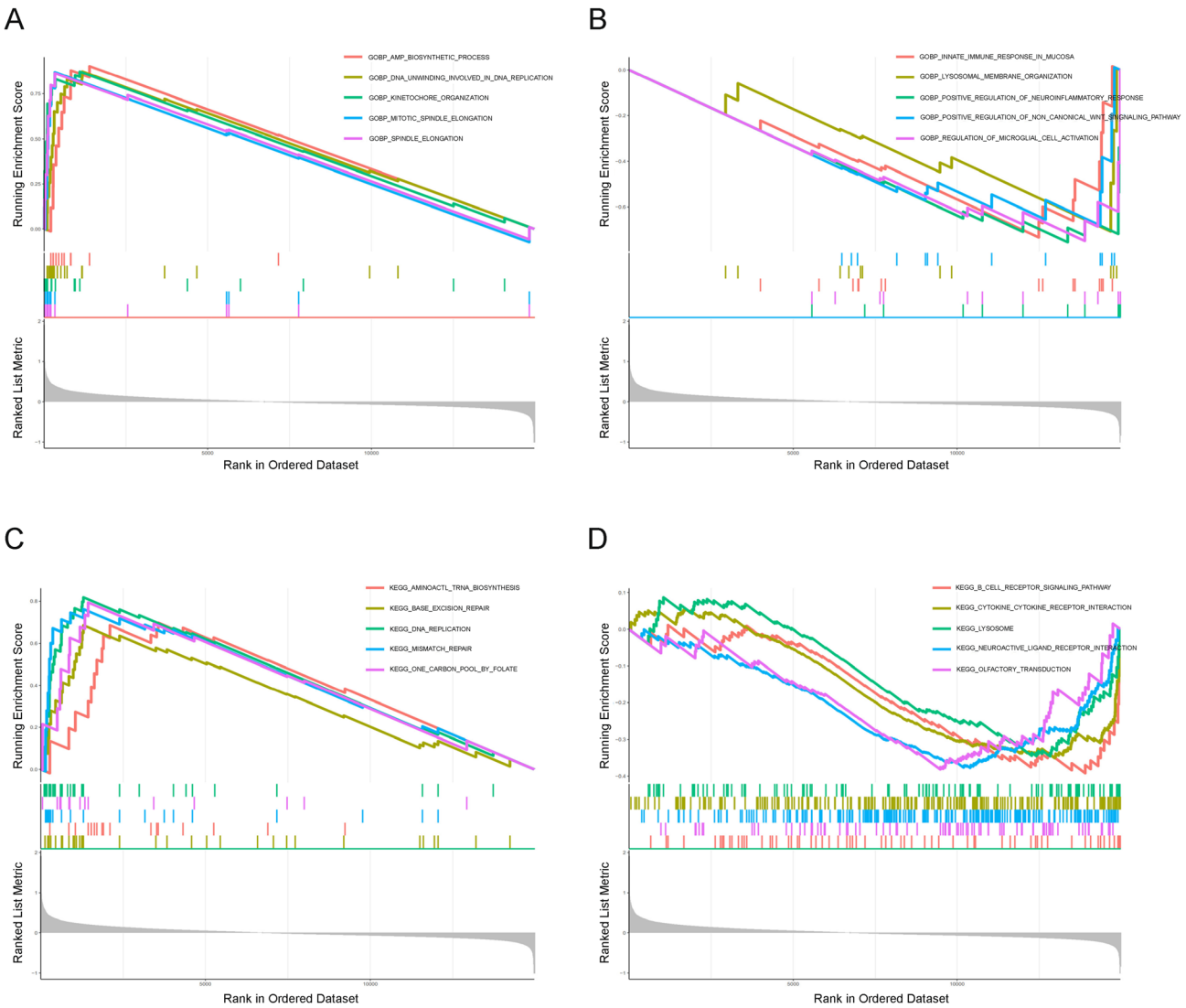

Fig. 6 Functional analysis of the gene expression profile between the NRGs low- and high-risk groups. **A** GO enrichments analysis of upregulated genes in the high-risk group. **B** GO enrichments analysis of upregulated genes in a low-risk group. **C** KEGG enrichment analysis of upregulated genes in the high-risk group. **D** KEGG enrichment analysis of upregulated genes in a low-risk group

Autologous stem cell transplantation (ASCT) is the preferred treatment for asymptomatic multiple myeloma patients under the age of 65, as well as for elderly patients whose physical condition allows for the procedure [42]. However, vincristine, doxorubicin, and dexamethasone are required before ASCT to prevent bone marrow transplantation from interfering with stem cell collection. Before the introduction of immune checkpoint inhibitors (ICIs), stage IV melanoma and some other solid tumors were treated very poorly because treatment options other than chemotherapy were very limited. The effective results of ICIs in solid malignancies led researchers to wonder if they could play the same role in hematologic malignancies [43]. The results achieved with ICIs in MM proved to be very promising, suggesting that ICI inhibitor therapy could be used as an adjuvant therapy in the clinic [44]. The prognostic signature we constructed suggests that ANXA1, ANXA2, HIF1A, HSPE1, MCOLN3, and FN1 are positively correlated with risk scores, suggesting that patients may be able to benefit from inhibitors of these genes. Conversely, blocking LYZ and FN1 may not yield significant results. In conclusion, additional long-term follow-up research is crucial to validate the safety and efficacy of ICIs for MM patients.

Although our nine-gene risk prognostic signature and nomogram provide new guidance for the prognosis of patients with MM, some limitations of this study remain. Firstly, a potential bias exists as the GEO database contains only patients from the USA and lacks data on patients from other countries. Second, due to the limitations of clinical specimens and experimental conditions, we did not design

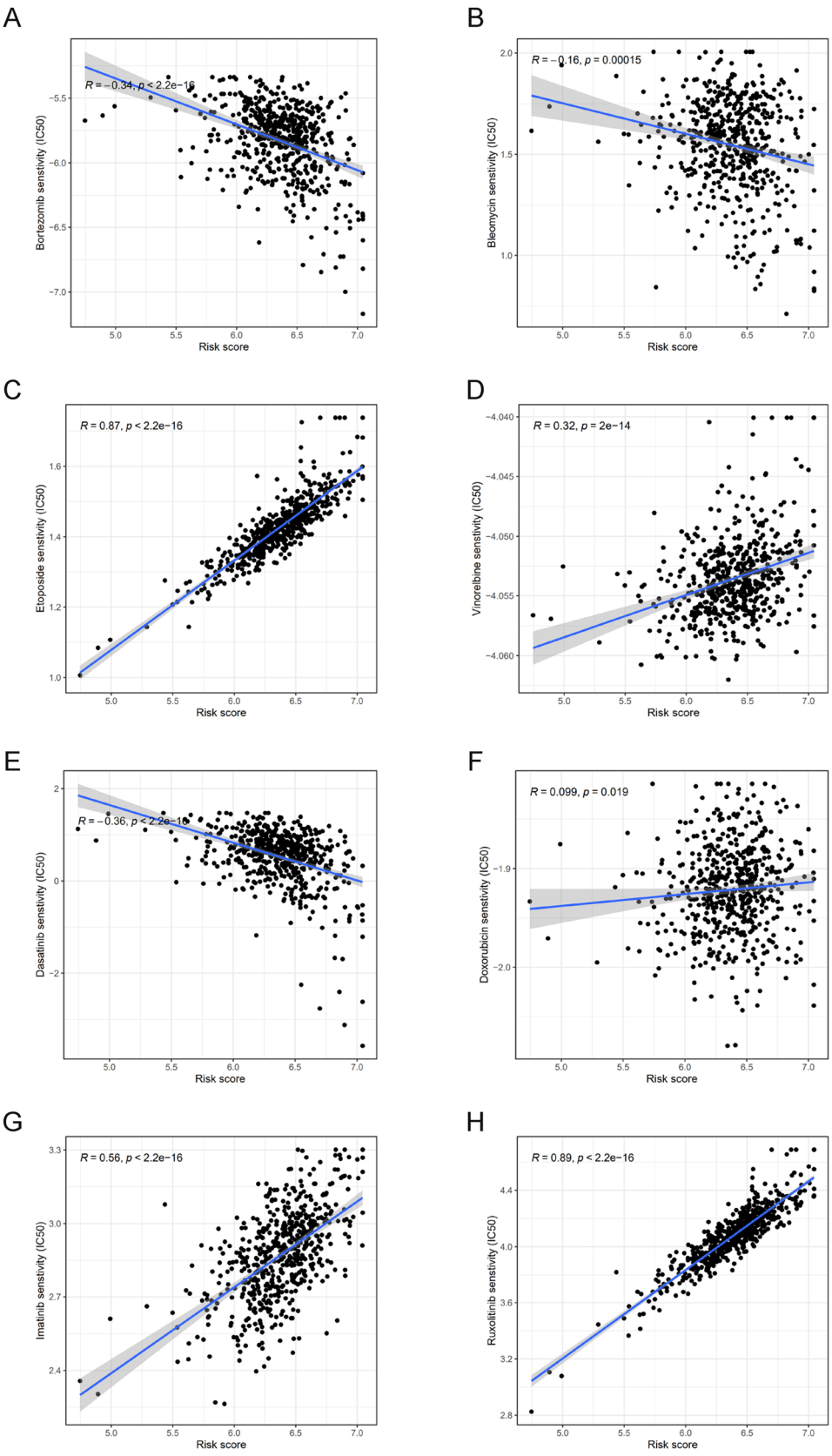

Fig. 7 Scatterplot of the relationship between prognostic gene expression and drug sensitivity

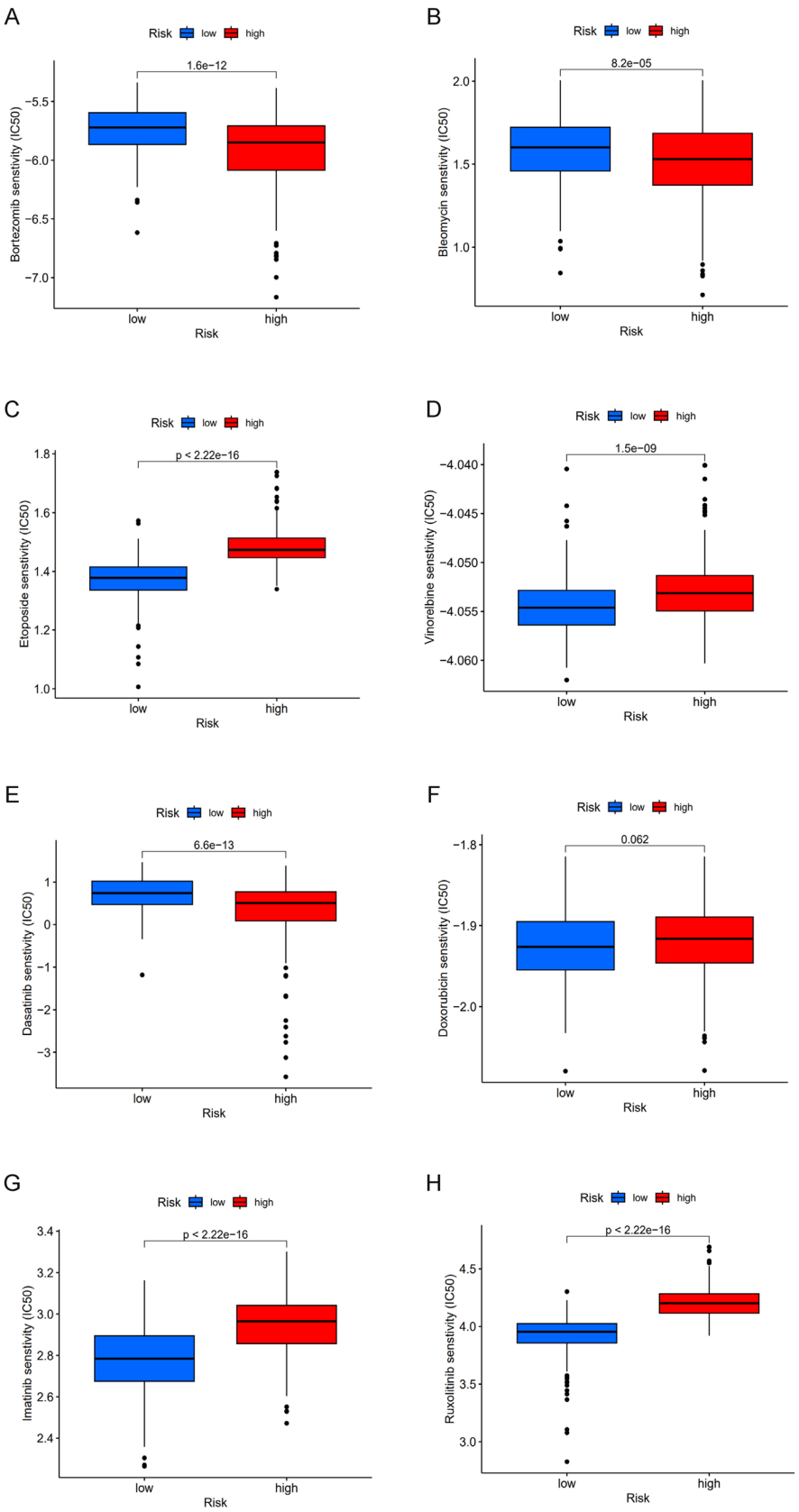

Fig. 8 Relationship between risk scores and treatment sensitivity

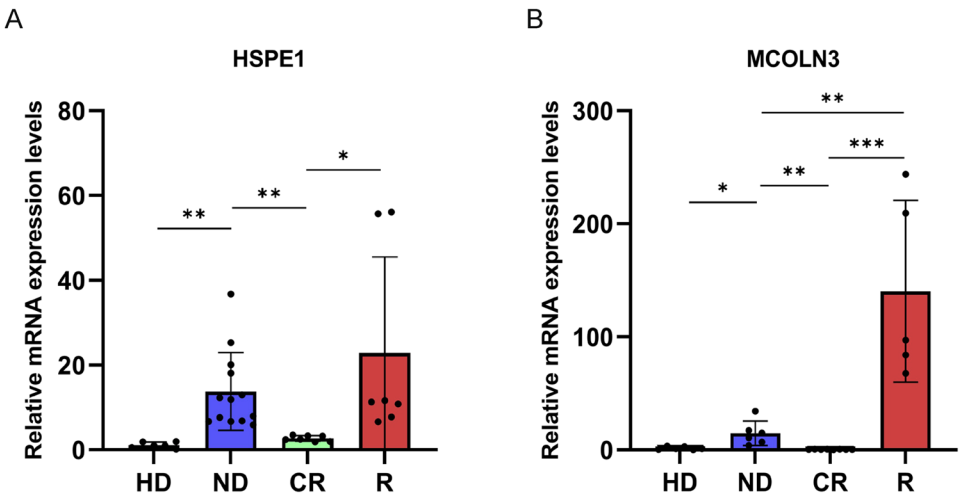

Fig. 9 Relative mRNA levels of the two NRGs were assessed by qPCR. **A** HSPE1. **B** MCOLN3. $^{*}p<0.05$, $^{**}p<0.01$, $^{***}p<0.001$

experiments to investigate the functions of the nine genes in MM-related signaling pathways. Moreover, our study proposes a novel prognostic signature based on NRGs, it is important to acknowledge that this model does not show significant improvement over the existing prognostic models in multiple myeloma (MM). Additionally, a potential limitation of our study is the lack of a ROS-related signature, which has been suggested to play a role in disease progression and therapy resistance in MM. While our focus was on NRGs, incorporating ROS-related biomarkers into future models could offer a more comprehensive understanding of the disease's underlying mechanisms and improve prognostic accuracy. Therefore, the mechanisms by which these nine genes affect the prognosis of MM patients need additional exploration.

Conclusion

In this investigation, we pinpointed novel genes associated with MM prognosis and established a prognostic signature comprising nine genes. This signature showed independent predictive capacity across both training and validation cohorts, successfully distinguishing between high-risk and low-risk patients, and offering a valuable tool for stratifying stage II multiple myeloma (MM) patients. Our study assessed the predictive capability of the risk signature and identified possible therapeutic medications.

Supplementary Information The online version contains supplementary material available at https://doi.org/10.1007/s10238-025-01692-1.

Acknowledgements We would like to thank the GEO database for the data and the editors and reviewers for their comments on this manuscript.

Author contributions QST and ZMZ conceptualized and designed the study. HTY and YYD collected the data. HPW, HQ, and WJD performed data analysis. HTY and YYD drafted the manuscript. All authors read and approved the final manuscript.

Funding This work was supported by grants from the Natural Science Foundation of Anhui province (No.2208085MH217) and the Research Fund of Anhui Institute of Translational Medicine (No. 2022zhyx-C51).

Data availability All data are available from the GEO (https://ncbi.nlm.nih.gov/geo/) database within the article. GEO database under accession numbers GSE2658 and GSE136337. The datasets used or analyzed during the current study are available from the corresponding author upon reasonable request.

Declarations

Competing interests The authors declare no competing interests.

Ethics approval and consent to participate.
This study was approved by the Ethics Committee of the Second Affiliated Hospital of Anhui Medical University, and informed consent was obtained from all patients. All experiments were conducted by relevant guidelines and regulations.

References

1. Dimopoulos MA, Moreau P, Terpos E, et al. Multiple myeloma: EHA-ESMO clinical practice guidelines for diagnosis, treatment and follow-up(†). Ann Oncol. 2021;32:309–22.
2. Durie BG, Salmon SE. A clinical staging system for multiple myeloma. Correlation of measured myeloma cell mass with presenting clinical features, response to treatment, and survival. Cancer. 1975;36:842–54.
3. Pawlyn C, Morgan GJ. Evolutionary biology of high-risk multiple myeloma. Nat Rev Cancer. 2017;17:543–56.
4. Schavgoulidze A, Cazaubiel T, Perrot A, et al. Multiple myeloma: heterogeneous in every way. Cancers. 2021;13:1285.
5. Kastritis E, Terpos E, Dimopoulos MA. How I treat relapsed multiple myeloma. Blood. 2022;139:2904–17.
6. Cristinziano L, Modestino L, Antonelli A, et al. Neutrophil extracellular traps in cancer. Semin Cancer Biol. 2022;79:91–104.
7. Xiong S, Dong L, Cheng L. Neutrophils in cancer carcinogenesis and metastasis. J Hematol Oncol. 2021;14:173.
8. Hedrick CC, Malanchi I. Neutrophils in cancer: heterogeneous and multifaceted. Nat Rev Immunol. 2022;22:173–87.
9. Ramachandran IR, Condamine T, Lin C, et al. Bone marrow PMN-MDSCs and neutrophils are functionally similar in protection of multiple myeloma from chemotherapy. Cancer Lett. 2016;371:117–24.
10. Lee KH, Kronbichler A, Park DD, et al. Neutrophil extracellular traps (NETs) in autoimmune diseases: a comprehensive review. Autoimmun Rev. 2017;16:1160–73.
11. Ria R, Catacchio I, Berardi S, et al. HIF-1α of bone marrow endothelial cells implies relapse and drug resistance in patients with multiple myeloma and may act as a therapeutic target. Clin Cancer Res. 2014;20:847–58.
12. Seckinger A, Meissner T, Moreaux J, et al. Clinical and prognostic role of annexin A2 in multiple myeloma. Blood. 2012;120:1087–94.
13. Shi H, Pan Y, Xiang G, et al. A novel NET-related gene signature for predicting DLBCL prognosis. J Transl Med. 2023;21:630.
14. D'Agostino M, Cairns DA, Lahuerta JJ, et al. Second revision of the international staging system (R2-ISS) for overall survival in multiple myeloma: a European myeloma network (EMN) report within the HARMONY project. J Clin Oncol. 2022;40:3406–18.
15. Marcon C, Simeon V, Deias P, et al. Expert's consensus on the definition and management of high risk multiple myeloma. Front Oncol. 2022;12:1096852.
16. Kyle RA, Rajkumar SV. Multiple myeloma. Blood. 2008;111:2962–72.
17. Spaan I, Raymakers RA, van de Stolpe A, Peperzak V. Wnt signaling in multiple myeloma: a central player in disease with therapeutic potential. J Hematol Oncol. 2018;11:67.
18. Zhang J, Wang C, Yu Y. Comprehensive analyses and experimental verification of NETs and an EMT gene signature for prognostic prediction, immunotherapy, and chemotherapy in pancreatic adenocarcinoma. Environ Toxicol. 2024;39:2006–23.
19. Mo G, Long X, Cao L, et al. A six-gene prognostic model based on neutrophil extracellular traps (NETs)-related gene signature for lung adenocarcinoma. Comb Chem High Throughput Screen. 2024;27:1969–83.
20. Xiao D, Zeng T, Zhu W, et al. ANXA1 promotes tumor immune evasion by binding PARP1 and upregulating Stat3-induced expression of PD-L1 in multiple cancers. Cancer Immunol Res. 2023;11:1367–83.
21. Calmon MF, Mota MT, Babeto É, et al. Overexpression of ANXA1 in penile carcinomas positive for high-risk HPVs. PLoS ONE. 2013;8: e53260.
22. Garcia Pedrero JM, Fernandez MP, Morgan RO, et al. Annexin A1 down-regulation in head and neck cancer is associated with epithelial differentiation status. Am J Pathol. 2004;164:73–9.
23. Milanovic M, Fan DNY, Belenki D, et al. Senescence-associated reprogramming promotes cancer stemness. Nature. 2018;553:96–100.
24. Wang J, He Z, Liu X, et al. LINC00941 promotes pancreatic cancer malignancy by interacting with ANXA2 and suppressing NEDD4L-mediated degradation of ANXA2. Cell Death Dis. 2022;13:718.
25. Mao L, Yuan W, Cai K, et al. EphA2-YES1-ANXA2 pathway promotes gastric cancer progression and metastasis. Oncogene. 2021;40:3610–23.
26. Wu Q, You L, Nepovimova E, et al. Hypoxia-inducible factors: master regulators of hypoxic tumor immune escape. J Hematol Oncol. 2022;15:77.
27. Chang YL, Yang CY, Lin MW, et al. High co-expression of PD-L1 and HIF-1α correlates with tumour necrosis in pulmonary pleomorphic carcinoma. Eur J Cancer. 2016;60:125–35.
28. Yang Y, Ding R, Wang R. Identification of candidate targets and mechanisms involved in miRNA regulation in multiple myeloma. World J Surg Oncol. 2022;20:23.
29. Bie AS, Fernandez-Guerra P, Birkler RI, et al. Effects of a mutation in the HSPE1 gene encoding the mitochondrial co-chaperonin HSP10 and its potential association with a neurological and developmental disorder. Front Mol Biosci. 2016;3:65.
30. Lei Y, Klionsky DJ. MCOLN3/TRPML3 bridges the regulation of autophagosome biogenesis by PtdIns3P and the calcium channel. Autophagy. 2023;19:377–8.
31. Cheng X, Shen D, Samie M, Xu H. Mucolipins: Intracellular TRPML1-3 channels. FEBS Lett. 2010;584:2013–21.
32. Kim HJ, Soyombo AA, Tjon-Kon-Sang S, et al. The Ca(2+) channel TRPML3 regulates membrane trafficking and autophagy. Traffic. 2009;10:1157–67.
33. Li J, Chen C, Chen B, Guo T. High FN1 expression correlates with gastric cancer progression. Pathol Res Pract. 2022;239: 154179.
34. Wang H, Zhang J, Li H, et al. FN1 is a prognostic biomarker and correlated with immune infiltrates in gastric cancers. Front Oncol. 2022;12: 918719.
35. Zhang XX, Luo JH, Wu LQ. FN1 overexpression is correlated with unfavorable prognosis and immune infiltrates in breast cancer. Front Genet. 2022;13: 913659.
36. Gu Z, Wang L, Dong Q, et al. Aberrant LYZ expression in tumor cells serves as the potential biomarker and target for HCC and promotes tumor progression via csGRP78. Proc Natl Acad Sci USA. 2023;120: e2215744120.
37. Devlin JC, Axelrad J, Hine AM, et al. Single-cell transcriptional survey of Ileal-anal pouch immune cells from ulcerative colitis patients. Gastroenterology. 2021;160:1679–93.
38. Wenzel J, Spyropoulos D, Assmann JC, et al. Endogenous THBD (Thrombomodulin) mediates angiogenesis in the ischemic brain-brief report. Arterioscler Thromb Vasc Biol. 2020;40:2837–44.
39. Weiler-Guettler H, Christie PD, Beeler DL, et al. A targeted point mutation in thrombomodulin generates viable mice with a prethrombotic state. J Clin Invest. 1998;101:1983–91.
40. Hosaka Y, Higuchi T, Tsumagari M, Ishii H. Inhibition of invasion and experimental metastasis of murine melanoma cells by human soluble thrombomodulin. Cancer Lett. 2000;161:231–40.
41. Suehiro T, Shimada M, Matsumata T, et al. Thrombomodulin inhibits intrahepatic spread in human hepatocellular carcinoma. Hepatology. 1995;21:1285–90.
42. Sirohi B, Powles R, Mehta J, et al. An elective single autograft with high-dose melphalan: single-center study of 451 patients. Bone Marrow Transplant. 2005;36:19–24.

43. Alkharabsheh O, Trisel Z, Badami S, et al. Checkpoint inhibitors in multiple myeloma: intriguing potential and unfulfilled promises. Cancers. 2021;14:113.
44. Tamura H, Ishibashi M, Sunakawa M, Inokuchi K. Immunotherapy for multiple myeloma. Cancers. 2019;11:2009.